

01 Jan 2022

Steel Diaphragm Innovation Initiative, Year 5, Final Report *Addendum*

American Iron and Steel Institute

Follow this and additional works at: <https://scholarsmine.mst.edu/ccfss-aisi-spec>



Part of the [Structural Engineering Commons](#)

Recommended Citation

American Iron and Steel Institute, "Steel Diaphragm Innovation Initiative, Year 5, Final Report *Addendum*" (2022). *American Iron and Steel Institute (AISI) Specifications, Standards, Manuals and Research Reports (1946 - present)*. 234.

<https://scholarsmine.mst.edu/ccfss-aisi-spec/234>

This Technical Report is brought to you for free and open access by Scholars' Mine. It has been accepted for inclusion in American Iron and Steel Institute (AISI) Specifications, Standards, Manuals and Research Reports (1946 - present) by an authorized administrator of Scholars' Mine. This work is protected by U. S. Copyright Law. Unauthorized use including reproduction for redistribution requires the permission of the copyright holder. For more information, please contact scholarsmine@mst.edu.

research report

Steel Diaphragm Innovation Initiative, Year 5, Final Report *Addendum*

RESEARCH REPORT RP22-01

January 2022



American Iron and Steel Institute

DISCLAIMER

The material contained herein has been developed by researchers based on their research findings and is for general information only. The information in it should not be used without first securing competent advice with respect to its suitability for any given application. The publication of the information is not intended as a representation or warranty on the part of the American Iron and Steel Institute or of any other person named herein, that the information is suitable for any general or particular use or of freedom from infringement of any patent or patents. Anyone making use of the information assumes all liability arising from such use.

PREFACE

The Steel Diaphragm Innovation Initiative (SDII) is a multi-year industry-academic-government partnership to advance the seismic performance of steel floor and roof diaphragms utilized in steel buildings. This addendum to the final report covers work conducted on Task 5.6 which was completed during a no-cost extension conducted in 2021. Please refer to AISI RP21-04, the *Steel Diaphragm Innovation Initiative, Year 5, Final Report* for all other details.

SDII

Steel Diaphragm Innovation Initiative

Year 5 Final Report ***Addendum***
(1 Jan 2021 – 31 December 2021)

Authors:

Lead Investigators

Matt Eatherton, Sam Easterling, Jerry Hajjar, Ben Schafer
Research Faculty and Staff, Postdoctoral Scholars

Shahab Torabian, Kyle Coleman

Graduate Students

Robert Bailey Bond, Nicholas Evans Briggs, Astrid Winther Fischer,
Hamid Foroughi, Raul Avellaneda Ramirez, Gengrui Wei

SDII Information

The Steel Diaphragm Innovation Initiative (SDII) is a multi-year industry-academic partnership to advance the seismic performance of steel floor and roof diaphragms utilized in steel buildings through better understanding of diaphragm-structure interaction, new design approaches, and new three-dimensional modeling tools that provided enhanced capabilities to designers utilizing steel diaphragms in their building systems. SDII was created through collaboration between the American Iron and Steel Institute and the American Institute of Steel Construction with contributions from the Steel Deck Institute, the Metal Building Manufacturers Association, and the Steel Joist Institute in partnership with the Cold-Formed Steel Research Consortium; including, researchers from Johns Hopkins University, Virginia Tech, Northeastern University, and Walter P Moore.

CFSRC Information

The Cold-Formed Steel Research Consortium (CFSRC) is a multi-institute consortium of university researchers dedicated to providing world-leading research that enables structural engineers and manufacturers to realize the full potential of structures utilizing cold-formed steel. More information can be found at www.cfsrc.org. All CFSRC reports are hosted permanently by the Johns Hopkins University library in the DSpace collection:

<https://jscholarship.library.jhu.edu/handle/1774.2/40427>.

Complete List of SDII Participants

Lead Investigators

Matt Eatherton, Sam Easterling (SDII Year 2-), Jerry Hajjar, Cris Moen, (SDII Year 1), Rafael Sabelli, Ben Schafer

Research Faculty and Staff, Postdoctoral Scholars

Paul Bergson (SDII Year 5), Kyle Coleman (SDII Year 2-), David Padilla-Llano (SDII Year 1 and 2), Shahab Torabian

Graduate Students

Pat O'Brien (SDII Year 1 and 2), Shaoning Li (SDII Year 2), Astrid Winther Fischer (SDII Year 2-), Basit Qayyum (SDII Year 2 and 3), Nicholas Evans Briggs (Year 3-) Hamid Foroughi (SDII Year 3-), Mithila Bhagavathi Madhavan (SDII Year 3-4), Raul Avellaneda Ramirez (SDII Year 3-), Yifei Shi (SDII Year 3), Gengrui Wei (SDII Year 3-), Robert Bailey Bond (SDII Year 4-5), Colin Hug (SDII Year 4), Abigail Desa (SDII Year 5), Bayley St. Jacques (SDII Year 5)

1 Summary

The Steel Diaphragm Innovation Initiative (SDII) is a multi-year industry-academic-government partnership to advance the seismic performance of steel floor and roof diaphragms utilized in steel buildings. This addendum to the final report covers work conducted on Task 5.6 which was completed during a no-cost extension conducted (1 Jan. 2021 – 31 Dec. 2021). See the final report for all other details.

5 Experiments: Project Completion

As discussed in the final report the building bay testing of Task 5.6 was conducted during a no cost extension year. Summary of that testing is provided in this addendum.

5.6 Building Bay/Full Building Tests

SDII Case and Plan, Experiments, Tasks 6 and 7, are focused on large scale testing. Outside funding was not secured for a full building test; however, the SDII team has conducted a large scale cyclic test of a full building bay at the STReSS Lab in Northeastern. This test rounds out the diaphragm testing pursued by SDII by including many of the features of actual building construction that are not captured in traditional diaphragm testing.

The test discussed in this section applies cyclic loading to a full-scale concrete-filled steel deck diaphragm specimen including the entire floor framing system with a column at each of the four corners and load applied in the center of the specimen, as depicted in Figure 1. This type of specimen differs from the commonly used cantilever diaphragm specimens, which assume a line of symmetry through the middle of the diaphragm, so that only one-half of the prototype diaphragm is constructed and includes only the “skin” of the diaphragm and known of the underlying framing. This specimen also follows standard construction practices that are prevalent in the United States, including the use integral pour stops. By constructing the specimen in this manner, a realistic understanding is provided for how a full-scale diaphragm built according to current standards could perform under seismic events.



Figure 1: Diaphragm Specimen Isometric

The design of the specimen was informed by SDII’s cantilever diaphragm database, recent SDII cantilever diaphragm testing, monotonic and cyclic push-out experiments, and the SDII building archetypes. The full-scale diaphragm bay specimen has been designed to emulate a portion of these well-informed building archetypes. Through mirroring member sizes, shear stud configuration and

size, deck geometry, reinforcement pattern, and lateral force resisting system (LFRS) flexibility, a specimen has been designed that represents much of the current composite (concrete-filled steel deck) floor diaphragms built today. The specimen consists of one 20 ft × 28 ft bay (center-to-center spacing) spanning between four W14×176 columns, as shown in Figure 2. Each column has two braces at its base. The perimeter of the diaphragm has two collectors fabricated from W18×35's spanning the shorter edge of the specimen and two chords made from W21×62's. There are three W21×62 girders running parallel to the collectors. Lastly there are four W16×26 beams which run parallel to the chords. These sizes were chosen based on the SDII building archetype designs. This helps to ensure that the specimen represents common construction practices and that the specimen matches normal building diaphragm behavior.

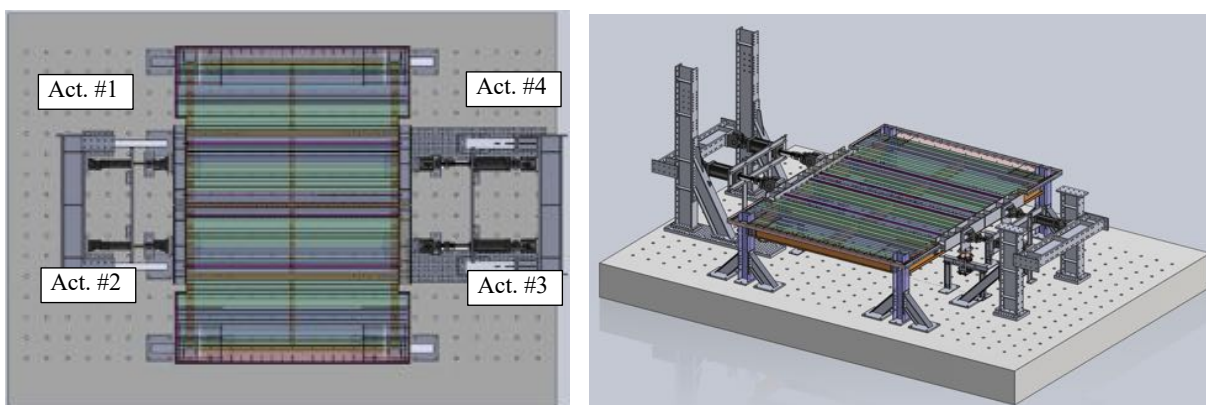


Figure 2 Full-scale diaphragm specimen plan and isometric views

The specimen includes 3 in. high steel deck with 3.25 in. of lightweight concrete above the deck. Welded wire reinforcement, 6x6 – W2.1/W2.1, is used throughout the slab, additional reinforcement is included in the edge overhangs and surrounding the columns. The shear studs used are 0.75 in. in diameter and 4.5 in. long. The studs along the collector were designed with a spacing of 24 in. such that the stud strength has a comparable strength to the calculated diaphragm shear strength. The 24 in. stud spacing along the collector is relatively wide, but common in practice. In the tests (as in real construction) the slab may also bear against the columns, thus failure in diaphragm shear (diagonal tension cracking in the concrete), not at the shear studs, is the expected failure mode.

The diaphragm specimen is situated between two pairs of actuators. On the left of Figure 2 two large actuators move in the same direction as the two medium sized actuators shown on the right of the figure. By having the actuator pairs work together in anti-symmetry a maximum load is able to be applied to the specimen. Due to the cyclic nature of the load application the actuators are required to impose compressive and tensile loads on the specimen. The actuators act on the line of intersection between the concrete slab and the top of flange surface on the chords. In compression, two distribution beams are loaded by the actuators and in turn apply load to both the chord and the concrete. In tension, the distribution beams are loaded by the actuators such that they pull on the chord. In addition, to assist in applying tension to the concrete slab, each distribution beam is attached to a pair of threaded reinforcing bars that extend through the slab and are anchored on the distribution beam on the far side of the slab.

The loading protocol for this specimen follows the unidirectional testing protocol outlined in FEMA 461 (FEMA, 2007). This protocol entails two cycles at each amplitude target with a 40% increase in magnitude between targets. A total of six cycles are required prior to the point at which initial damage is expected. The four actuators were controlled to follow a control scheme that imparts a symmetrical displacement on the specimen. Large actuator #4 and medium actuator #2 were initially run in displacement control with the same displacement target (equal and opposite, as one actuator was pulling when the other was pushing); see Figure 2 for actuator identification. Medium actuator #1 and large actuator #3 were run in force control, receiving their force signal as the negated value from actuators #4 and #2, respectively. The force control used factors of 2.168 and 0.461 to adjust the force value coming from actuators #2 and #4, respectively due to the variation in actuator capacities between the medium and large actuators. This control scheme ensures the North and South portions of the specimen are loaded with the same displacements, but the resulting forces may differ. While the protocol was designed using FEMA 461 and the control scheme described was followed initially, some adjustments were made during the test, as static specimen strength eventually exceeded the loading capacity of the actuators (810 kips) and additional cycling of the specimen was necessary to induce failure.

The loading protocol followed for the diaphragm test is presented in Table 1. Laid out in this table are the displacement targets and the shear angles that result between the actuators loading point on the specimen (based on the actuator displacement value) and the centerline of the adjacent column. In the table it is specified whether or not the actuator displacement target is successfully reached in the West and East directions during the testing. Note that in each cycle, the specimen was loaded in the West direction first. The table also identifies which control scheme was used; either the original control scheme, described above, or an adapted (force) control scheme that was used later in the test. The adapted control scheme was implemented during the test when it was identified that the original control scheme was limiting the force that was being imparted to the specimen. The adapted control scheme used just actuator #4 in displacement control, with all three other actuators receiving their force values from actuator #4. This results in symmetric loading of the specimen, with possible unsymmetric displacement values being imposed on North and South portions of the specimen. Also identified in Table 1 is whether one or two factors are used in each cycle of the loading history. This refers to the factors imposed on the primary/secondary relationship between the actuators. The 2.168 and 0.461 values, as discussed above, represent one value, as they are inverses of each other. This factor is optimized for loading in the East direction, as it used the full capacity of both the medium and large actuators. To ensure symmetry in the loading at the peak value of each cycle, this factor was originally used in both directions. However, when it was determined that additional load was required, the original factors were used when loading in the East direction, and an alternative 0.304 factor was introduced for loading in the West direction. Later in the test, the two factors were alternated between when loading the specimen in the West and East directions at each cycle

Table 1: NEU Diaphragm Loading Protocol

Day	Displacement Step	# of Cycles	# of Ramps	Shear Angle, γ [-]	Actuator Displacement Target, δ [in]	Rate [in/min]	Control Scheme Used	Factor Used	Reached West Target	Reached East Target
Day 1	1	2	8	0.000191678	0.023	0.125	Original	One	Yes	Yes
	2	2	8	0.000268349	0.032	0.125	Original	One	Yes	Yes
	3	2	8	0.000375689	0.045	0.125	Original	One	Yes	Yes
	4	2	8	0.000525964	0.062826455	0.125	Original	One	Yes	Yes
	5	2	8	0.00073635	0.087957037	0.125	Original	One	Yes	Yes
	6	2	8	0.00103089	0.123139852	0.125	Original	One	Yes	Yes
	7	2	8	0.001443246	0.172395793	0.125	Original	One	Yes	Yes
	8	2	8	0.002020545	0.24135411	0.125	Original	One	Yes	Yes
	9	2	8	0.002828763	0.338	0.125	Original	One	Yes	No
	10	4	16	0.003960268	0.473	0.125	Original	One	No	No
	2	8	Original				Alternate	No	No	
Day 2	11	2	8	0.003114274	0.372	0.125	Original	One	Yes	No
	12	1	4	0.000375689	0.045	0.125	Adapted	One	Yes	Yes
	13	2	8	0.002828763	0.338	0.125	Adapted	One	Yes	Yes
	14	4	16	0.003960268	0.473	0.125	Adapted	One	Yes	Yes
	15	2	8	0.005544376	0.662	0.125	Adapted	Alternate	Yes	No
	16	8	32	0.007762126	0.927	0.25	Adapted	Alternate	No	No
Day 3	17	1	4	0.00366/-0.00396	+0.437/-0.473	0.125	Adapted	Alternate	Yes	Yes
Day 4	18	11	44	0.007762126	0.927	0.25	Adapted	Alternate	Yes	No
Day 5	19	5	20	0.010866976	1.298	0.25	Adapted	Alternate	Yes	Yes
Day 6	20	1	4	0.010866976	1.298	0.25	Adapted	Alternate	Yes	Yes
	21	2	8	0.015213767	1.817	0.5	Adapted	Alternate	Yes	Yes
	22	1	4	0.021299274	2.544	0.5	Adapted	Alternate	Yes	N/A

The observed diaphragm response differed across the four 7 ft × 20 ft bays that comprised the floor. For reference the bays are numbered 1 through 4 starting with the bay that is furthest to the North, and moving South (North is at the top in Figure 2a and on the right in Figure 4). Their differing behavior was partially due to differing concrete strength in these bays. Bays 1 and 4 should have experienced the most damage, as they have the maximum shear and span between the loaded section of the diaphragm and the columns. Conversely, Bays 2 and 3 have a loading beam across their width that stiffens them and allows the distribution of load from the actuators. However due to variation in the concrete pour, Bay 4 ended up with significantly stronger concrete compared to Bay 1. Figure 3 provides to total applied force vs. measured shear angle across the 4 bays of the specimen. In Figure 3 deformation is mainly concentrated in the end bays: 1 and 4, with significantly more deformation and finally failure occurring in Bay 1. The force in Figure 3 is the total load applied to the specimen. The maximum and minimum force values, approximately 810 kips when loading to the West and -615 kips when loading to the East, represent the combined actuator capacity rather than the ultimate static strength of the specimen. Failure occurred at the maximum force value through cycling as depicted in Figure 2.

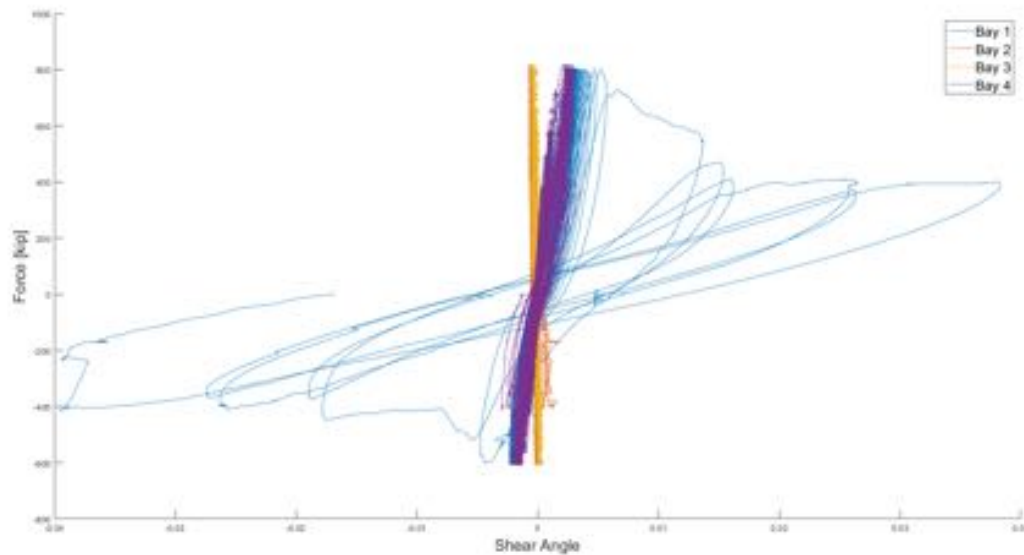
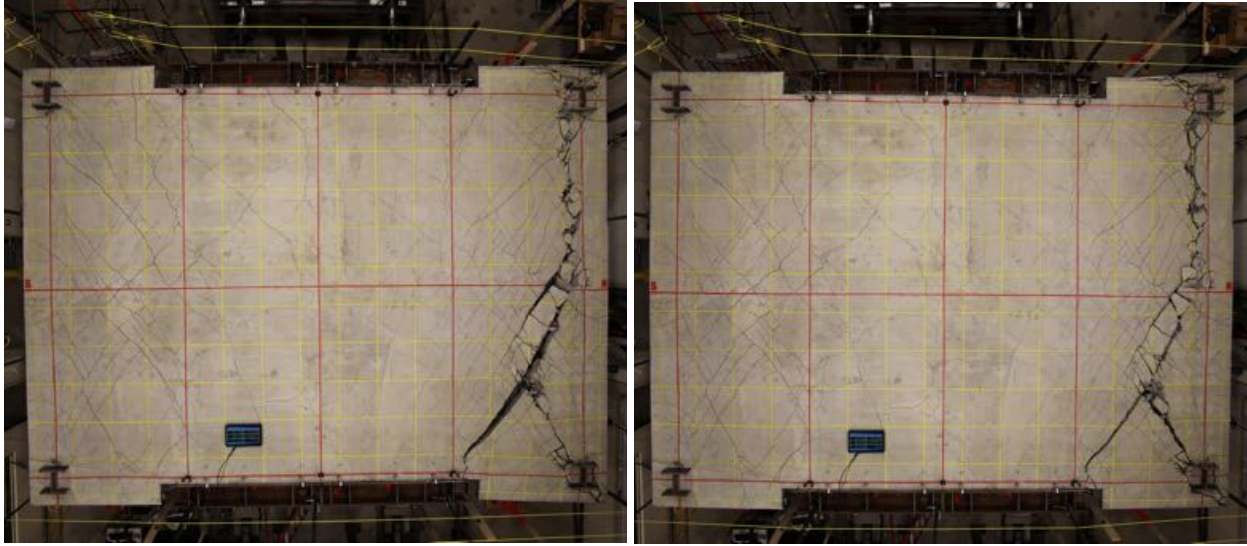


Figure 3: Hysteresis Results of Shear Angle of the Four Diaphragm Bays

While both end Bays 1 and 4 exhibited significant damage (particularly concrete cracking) as expected, failure in the specimen was eventually localized in the weaker concrete located in Bay 1 as shown in Figure 4. Figure 4a depicts the performance of the specimen at the peak deformation reached in the West direction and Figure 4b depicts the peak deformation reached in the East direction. Damage is concentrated in Bay 1, with significant concrete cracking in Bay 4. Bay 1 exhibits diagonal tension cracks in the concrete, especially on its East side. On the West side of Bay 1, cracking was initially in diagonal patterns, similar to Bay 4; however, failure ultimately occurred in the concrete with significant cracks reorienting to run somewhat parallel to the collector, but off of the line of shear studs. Extensive damage to the steel deck also occurred in Bay 1 subsequent to the concrete failure. Similar to the failure exhibited in the concrete, the steel deck on the East side of Bay 1 exhibited buckling and out-of-plane damage, whereas the steel deck on the West of Bay 1 exhibited seam failure directly below the line of concrete failure.

The static specimen strength exceeded the combined actuator strength of 810 kips and greatly exceeded the governing design strength. The specimen strength is estimated to be 547 kips using measured material properties and assuming the diagonal tension cracking failure mode (Eatherton et al., 2020) as recently adopted in AISI S310 based on full-scale cantilever diaphragm tests. Overall, the large strength of this specimen, well above typical predictive strengths used for design, exhibits additional aspects of performance that would be expected to increase strength in indeterminate concrete-filled steel deck diaphragms. These include the influence of the concrete bearing on the column face, the influence of framing beams on overall deformation, and the confining effects of the pour stops (and potentially edge reinforcing), which were left on during testing. Note, The static strength is higher than 810 kips, as the specimen underwent 19 cycles at a drift angle of 0.0078 before degrading strength during the next 0.0109 maximum drift angle cycles.



a) Specimen Loaded 2.544" West

b) Specimen Loaded about 2.4" East

Figure 4: Diaphragm Failure Mechanism

Conclusion of the testing constitutes the formal end to Task 5.6. However, significant additional post-processing and comparisons to design calculations will be conducted in the future. Using the extensive sensor network installed in the specimen the researchers intend to provide direct insight on the force flows in the diaphragm including understanding the amount of load shed directly to the columns and the progression of damage in typical concrete-filled steel deck diaphragms subjected to seismic loads. Special attention will be paid to using the sensor information to better understand the cyclic behavior of the crucial composite interface between the deck and the collectors. Additionally, this experiment allows the characterization of diaphragm ductility considering full floor framing rather than in isolation, an integral purpose of the SDII project, and necessary to further validate and improve ductility-based diaphragm design provisions. Additionally, with the completion of this experiment, there are further research opportunities to design and optimize concrete-filled steel deck diaphragms under seismic loads.

9 Acknowledgments

In addition to the acknowledgments in the final report the SDII team at Northeastern would like to thank the following companies for in-kind support Capone Iron, Fastenal, Hilti, Nelson, Nucor, Turner, and Verco Decking, Inc. Any typos, opinions, findings, recommendations, or other material within are those of the authors and do not necessarily reflect the views of the sponsors.

References

References added for this addendum include:

- Eatherton, M. R., O'Brien, P. E., & Samuel Easterling, W. (2020). Examination of Ductility and Seismic Diaphragm Design Force-Reduction Factors for Steel Deck and Composite Diaphragms. *Journal of Structural Engineering*, 146(11), 04020231.
- FEMA (2007). *FEMA 461: Interim Testing Protocols for Determining the Seismic Performance Characteristics of Structural and Nonstructural Components*. Washington D.C.: Federal Emergency Management Agency.



American Iron and Steel Institute

25 Massachusetts Avenue, NW
Suite 800
Washington, DC 20001

www.steel.org

